

Classification of EMG Signals: Using DWT Features and ANN Classifier

Karim M. Aljebory*, Yashar M. Jwmah, and Thabit S. Mohammed

Abstract— This study offers a concise overview of classifying hand movements based on their kinetic and myoelectric characteristics. In this work, we propose utilizing Electromyography (EMG) signals to distinguish these movements, especially for applications like wheelchair guidance and prosthetic control. Unlike prior research on forearm-derived EMG signals, this study employs a multi-channel surface Electromyography (sEMG) signal to effectively categorize distinct movements, crucial for prosthetic control.

To extract informative signal features, a two-step process is deployed, beginning with the transformation of raw EMG data using Discrete Wavelet Transform (DWT) for feature extraction. The ensuing classification task employs an Artificial Neural Network (ANN), overseen by the generation of corresponding confusion matrices (CMs) based on input features. The efficacy of our approach is validated using a human hand EMG signal dataset sourced from the UCI Machine Learning Repository. This dataset encompasses recordings from 36 subjects across 8 channels (sensors), spanning multiple days.

The suggested algorithm utilizes unprocessed bipolar EMG data for both training and evaluating the performance of the neural network-based classifier. Significantly, when assessing the algorithm's performance offline, it becomes evident that the use of Frequency Domain (FD) features in sequential signal processing outperforms Standard Linear Discriminant Analysis (LDA) algorithms. The combination of the DWT and ANN results in significantly improved performance and sustained robustness of the classification algorithm. Empirical findings prove the effectiveness of this approach, achieving an accuracy of 89.9% in classifying seven distinct hand movement categories accurately. Additionally, the analysis shows an increasing classification accuracy as the dataset size increases.

Index terms— Electromyography (EMG), Pattern Recognition, Feature Extraction, Signal Classification, Artificial Neural Network (ANN) Classifier, Prosthetic Hand.

I. INTRODUCTION

MANY people across the global landscape have experienced the loss of body parts, particularly hands or fingers, due to various circumstances, including hostile conflicts, wars, or accidents (such as those involving

warfare, automobiles, and industrial settings). For instance, Iraq has seen a rising population facing upper limb dysfunction, ranging from elbow impairments to complete upper digit amputations [1]. To address the challenges inherent in their daily lives, a critical need arises to furnish most of them with prosthetic devices. It's unfortunate, that the existing array of prosthetic devices remains limited in its ability to fully mimic human hand movements since they have a small set of gestures. Among the most promising techniques nowadays for handicapped persons is EMG-based control, in which the EMG signals can be utilized for these applications. By utilizing this technique, it is possible to control prostheses [1–3].

The EMG signal recognition process comprises two main phases: the extraction of specific signal features and the recognition of classes corresponding to specific hand movements. These processes are interrelated and rely on a preprocessing stage, as depicted in Fig. 1.

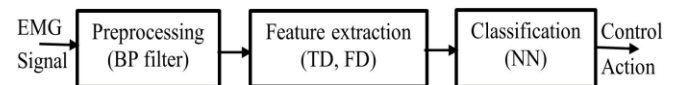


Fig. 1. Movement intention recognition block diagram.

However, grappling with hand movement presents intricate control challenges, attributed to several practical factors. Amongst such factors is that EMG signals are usually of small amplitude for finger and hand movements. The second considerable reason is linked with the muscles controlling the movements, which are located in the intermediate and the deep layers of the forearm. Furthermore, signals recorded behind the skin surface undergo different non-linear attenuations and filtering deformations by forearm tissues. As a consequence of these factors, more processing power might be needed to provide enough information to resolve ambiguity in the intended movement [4, 5]. In modern life, we can mention several tasks as being complicated and hence requiring skilled and dexterous control to achieve an efficient performance. Such tasks may include; driving a wheelchair, using a computer mouse, and operating contemporary devices like mobile phones, and other similar devices.

In this study, we conducted a pilot study with 36 participants who have upper limb deficiencies. These participants were instructed to perform significant movements for capturing wrist actions, including flexion, extension, and more[6]. Human hand motion control stems naturally from innate neural network impulses, which stimulate muscle contractions. To replicate and govern artificial hand movements using these impulses, a sophisticated bio-interfacing approach is needed. The change

Manuscript received Oct 4, 2022; revised Oct 9, 2023. This work was conducted as part of the cooperative program between the Ministry of Health and Environment of Iraq, Kirkuk Health Directorate, and AL-Qalam University College, Kirkuk, Iraq.

Karim M. Aljebory is an associate professor at the technical computer engineering department at AL-Qalam University College, Kirkuk, Iraq. (phone: +9647730666554; email: karim.eng@alqalam.edu.iq).

Thabit S. Mohammed is an associate professor at the computer technical engineering department at AL-Qalam University College, Kirkuk, Iraq. (email: thabit.sultan@alqalam.edu.iq).

Yashar M. Jwmah is a biomedical engineer at Kirkuk Health Directorate, Ministry of Health and Environment of Iraq (email: agronabaat@gmail.com).

in the electric potential difference between the interior of each stimulated muscle cell and its immediate environment measured on the skin's surface, accompanies the muscular engagement. Consequently, the information carried within EMG signals, indicative of muscle activity, is characterized by significant ambiguity, thereby sophisticating the precise analysis and discernment of the signals.

So, the information on muscle activity carried by EMG signals has much ambiguity, which sophisticates the appropriate analysis and recognition of these signals. The muscles controlling the hand fingers and wrist are located in the forearm and they are usually persevering even subsequent to hand amputation. [7–9].

This paper focuses on the extraction of high-effect signal features and implements a powerful classification technique using the Matlab software package as a tool for data analysis. A sequence of EMG signals is prompted by various hand movements from a typical subject to construct the adopted gesture datasets. For the testing and classification processes, the datasets from the UCI machine learning repository are adopted. These datasets were collected by eight sensors, which are integrated into the structure of the MYO armband. The armband encompasses eight EMG sensors that measure muscle tension, and an inertial measurement unit equipped with a 3D gyroscope, 3D accelerometer, and magnetometer [10],[11]. The myographic signals are simultaneously sent through a Bluetooth interface to a computation unit.

The armband's performance is illustrated by a series of EMG signals captured for a hand at rest, as in Fig. 2. This set of EMG signals is quite possible for an analysis tool such as; Fourier Transform (FT) and Wavelet Transform (WT) to be used for the extraction of many important features. The WT is particularly can deliver comprehensive information about signal features, so it is highly competitive in this context.

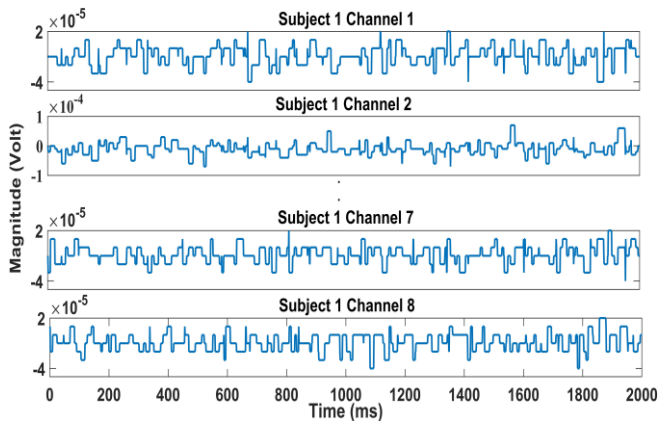


Fig. 2. EMG time-domain signals (class: hand at rest).

By processing an EMG signal, it is possible to classify different hand motions assigned to that particular signal. These motions are essential for human-machine interface in extensive applications spanning from upper limb and prosthesis control to robotic manipulation. Since the EMG signals are quasi-stochastic, within the 0 to 6 mV range and a frequency of 10 to 500 Hz may be contaminated by measurement noise [12]. The first step of processing is removing or mitigating this noise. This termed preprocessing, primarily focuses on accentuating the prominent attributes of the EMG signals, often achieved through the application of Fast Fourier Transform (FFT) and Discrete Wavelet

Transform (DWT) algorithms. The classification process is the last step, which is preceded by extracting a set of selected features that are considered in recognizing the corresponding movement pattern.

This paper is organized as follows; The current section provides a general preview of the fundamental properties of EMG signals, processing steps, and their role in driving artificial prosthetic devices. The next section conducts a comprehensive literature review, presenting key researchers who have contributed significantly to this field. Furthermore, specific research papers supporting the advancement of EMG signal classification within this study are examined.

Section III describes the adopted dataset in detail, along with an analysis of both the Time Domain (TD) and Frequency Domain (FD). This analysis helps select optimal preprocessor and filtering parameters. Section IV focuses on the proposed classification algorithm steps, providing a detailed description of the processes. Section V presents the experimental results obtained by testing the system's performance in the training, testing, and validation stages. Finally, Sections VI and VII offer the concluding remarks, discussion, conclusion, and future research directions.

II. LITERATURE REVIEW

In related literature, numerous researchers have made significant contributions to the classification of hand movements for the control of dexterous hand prosthetic devices using electromyography (EMG) signals. Jiang et al. [12] undertook the classification of six finger movements using four EMG channels combined with WT for feature extraction and classification. In [13], Naik et al. used the fractal dimension features and Independent Component Analysis (ICA) to identify four combinations of finger movements. In another study, AL-Timemy et al. [14], achieved the classification of 12 finger movements based on extracting the TD features of EMG signals provided by 16 unipolar electrodes, enhanced by a genetic algorithm as an optimizer and a support vector machine for classification. Sebelius et al. [15], and Pons et al. [16], introduced control strategies for virtual hand prostheses that hinged on varying classification algorithms. These methodologies utilize data gloves on healthy hands as references to train systems, enabling the performance of natural movements with the aid of virtual (computer-animated) hands as target tools. A control scheme for virtual hand prostheses, using different classification algorithms, was presented. The data glove on the healthy hand is used as a reference to train the system for performing natural movements with the aid of a virtual (computer-animated) hand as the target tool. Meanwhile, Herle et al. [17], presented a system to assist the patient in moving his upper limb by classification technique of surface electromyographical signals. Their architecture is based on feed-forward NN with 2 hidden layers, achieving a recognition rate of 96.67%. In their publications, Keles A.D. and Yucesoy C.D. [18], Lamounier, and Lopes [19], and Fernando E. R. Mattioli et al. [20], directed their efforts toward the development of a controller for virtual arm prostheses. In which, the EMG signal feature extraction and classification were considered common challenges. An ANN approach is a candidate to handle the classification problem.

In their research entitled “EMG-Based Feature Extraction and Classification for Prosthetic Hand Control”, Azhiri et al. [21] addressed their work to improve the accuracy of the classification process. A new set of five feature extraction functions at each level of DWT was used in conjunction with a postprocessing approach using NNs. Compared with conventional postprocessing methods such as; majority voting and Bayesian fusion methods, the proposed method achieves higher accuracy and better consistency.

Lobov et al. [22] intensively studied the latent factors and systematically determined the performance of surface EMG signal interfaces. They developed a procedure to quantify gesture fidelity in dynamic gaming environments. The user experience was tested in scenarios close to real ones, while the interface performance is measured in a gaming environment.

III. DATASETS DESCRIPTION AND PROCESSING

Data Description: The utilized dataset of surface electromyography (sEMG) was acquired and made publicly available online, hosted by the Physiobank repository at the UCI Institute [23]. This dataset comprises recordings from 36 individuals, each equipped with eight sensors on their forearm, and these recordings were conducted on two separate occasions. The recorded signals originate from the forearm muscles and correspond to seven distinct motion classes, denoted as; M1- hand at rest, M2- hand clenched in a fist, M3- wrist flexion, M4- wrist extension, M5- radial deviations, M6- ulnar deviations, M7- extended palm as depicted in Table I

TABLE I
RECOGNITION SCORE LABELS OF OUTPUT LAYER

Hand motion	Image	Outputs score						
Hand at rest (M1)		0	0	0	0	0	0	0
Hand clenched in a fist (M2)		1	0	0	0	0	0	0
Wrist flexion (M3)		0	1	0	0	0	0	0
Wrist extension (M4)		0	0	1	0	0	0	0
Radial deviations (M5)		0	0	0	1	0	0	0
Ulnar deviations (M6)		0	0	0	0	1	0	0
Extended palm (M7)		0	0	0	0	0	0	1

Each gesture signal was recorded within a maximum timeframe of 3 seconds and repeated twice, subsequently digitized into a stream of guaranteed samples covering the entire range of motions. The raw data for each class is presented in a tabulated series of 8 columns for sensor readings and 1 column for the measuring timestamp. The context is the EMG signal amplitude ranged from (-3×10^{-5}) to (3×10^{-5}) volts. Referring to the International Society of Electrophysiology and Kinesiology (ISEK), the filtering parameters are; low frequency (~ 5 Hz), and high frequency (~ 500 Hz) which ensures information saves[24]. The measured data is reorganized into a three-dimensional matrix of 2000 instants * 8 channels * 36 cases and the unmarked data was removed because they don't reveal information.

Data Processing: A practical analysis of FFT for the EMG revealed that a band-pass (BP) filter of (3-200Hz) frequency range saves the important features embedded in the signals. The basic filtering procedure is autoregressive in nature with generalized discrete-time domain transfer function $H(z)$ by cascading low-pass and high-pass filters. The transfer function of the filter is derived from a difference equation, and expressed in the Z-domain as follows; [23, 25, 26].

$$H(z) = \frac{Y(Z)}{X(Z)} = \frac{\sum_0^N b_n Z^{-n}}{\sum_0^M a_m Z^{-m}} = \frac{b_0 + b_1 z^{-1} + b_2 z^{-2} + \dots + b_N z^{-N}}{a_0 + a_1 z^{-1} + a_2 z^{-2} + \dots + a_M z^{-M}} \quad (1)$$

The symbols a_k , and b_k stand for the autoregressive and the moving-average coefficients, respectively. The expression in equation (1) can be simply decomposed into what is called *second-order sections*.

$$H(z) = \prod_1^L \frac{b_{0k} + b_{1k} z^{-1} + b_{2k} z^{-2}}{1 + a_{1k} z^{-1} + a_{2k} z^{-2}} \quad (2)$$

Equation (2) can be readily integrated into digital computing systems. The filter transfer function $H(z)$ is represented in a transition matrix (A) comprising 6 columns corresponding to the numerator (3bk) and denominator (3ak) coefficients, while L rows represent the Second-Order Sections of the Infinite Impulse Response (IIR) Filter;

$$A = \begin{bmatrix} b_{01} & b_{11} & b_{21} & 1 & a_{11} & a_{21} \\ b_{02} & b_{12} & b_{22} & 1 & a_{12} & a_{22} \\ \vdots & \vdots & \vdots & \vdots & \vdots & \vdots \\ b_{0L} & b_{1L} & b_{2L} & 1 & a_{1L} & a_{2L} \end{bmatrix} \quad (3)$$

The filter order denoted as L, specifies the response and behavior of the filter. Once the desired filter modules have been designed, the Second-Order Section Filters can be directly simulated by MATLAB for any chosen value of L. In Fig. 3, we present the frequency response of a specific filter, characterized by parameters (fs = 1 kHz, and L=236) as a test illustrating the filter's performance.

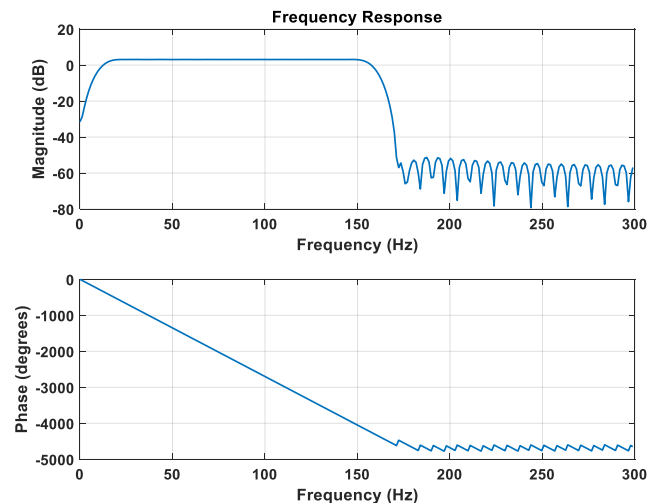


Fig. 3. The BP (5-160 Hz) filter frequency spectrum.

A comprehensive assessment of the hand's sEMG signal data, employing Fast Fourier Transform (FFT) analysis and drawing upon findings from numerous published sources [29], has affirmed that an empirical band limit range of 3 to 180 Hz stands as the optimal choice for a band-pass filter.

A practical evaluation of the hand's sEMG signal based on the FFT analysis and results in many published literature [27], proved that an empirical band limit value of (3-180 Hz) is optimal for a band-pass filter that saves the essential information needed for movement recognition.

The filtered signals exhibit minimal high-frequency noise and unneeded data (unmarked data). The frequency band of the filter in equation (1) has been systematically explored across multiple values for the 8 channels. The selection of the filter parameters is based on the entropy within a moving window of the signal. A window of 10 Hz length is adopted and the stop band frequency is determined when the entropy of the window falls below 0.0001 of the maximum signal entropy value. For demonstration purposes, the time spectrum for a filtered signal is shown in Fig. 4.

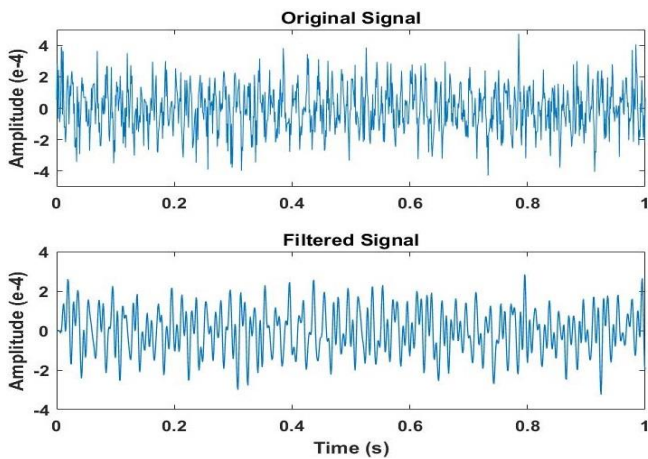


Fig. 4. The time spectrum of the BP-filtered EMG signal (channel 1).

Feature Extraction Using DWT: The DWT provides an effective method for analyzing nonstationary signals by decomposing them into different scales. This process entails breaking down the signal of interest into a set of multi-resolution coefficients, allowing us to unveil various facets of the signal, such as trends, discontinuities, and recurring patterns. For these reasons, the DWT is injected into the proposed algorithm to categorize an unknown signal feature classification. The DWT extracts the characteristics of the signal in both time and frequency domains by a scaling function and a wavelet function. This decomposition process results in two distinct components: the approximation component and the detail component, both of which carry valuable information from the original time series data.

For real-time applications, the DWT is recommended for non-stationary signals. By DWT, it is possible to analyze the signal at low frequencies and to observe the global information of the signal in high frequencies. The DWT enables multi-level decomposition of a signal by using filter banks $h[n]$ and $g[n]$, where the output of the low-pass filter is called as approximate coefficient and the output of the high-pass filter is a detailed coefficient. To compute the DWT coefficients, for an input signal $x[n]$, the filter banks consist

of a high-pass $h[n]$ and a low-pass filter $g[n]$, followed by down sampling by a factor of two. This is performed to compute both the detail and the approximation respectively as in Fig. 5. Specifically, the result from the low-pass filter corresponds to the approximate coefficient, while that from the high-pass filter corresponds to the detailed coefficient. Furthermore, for extensive decomposition, it is possible to cascade multiple stages [28–30].

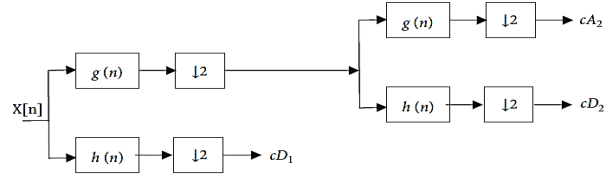


Fig. 5. Multi-level decomposition in DWT

The mathematical representation of the decomposition process of a discrete input signal $x[n]$, is described by equation (4).

$$x[n] = \sum_k a_{i,k} \phi_{i,k}[n] + \sum_{j=i}^{J-1} \sum_k d_{j,k} \psi_{j,k}[n] \quad (4)$$

Where a, d are the approximation and detail coefficient respectively, $i = j_0$, $\Psi[n]$ is the mother wavelet, and $\phi[n]$ is the scaling function defined by;

$$\psi_{j,k}[n] = 2^{\frac{j}{2}} \Psi(2^j n - k)$$

$$\phi_{i,k}[n] = 2^{\frac{i}{2}} \phi(2^i n - k)$$

The DWT algorithm is carried out by sequentially passing the EMG signal through high-pass and low-pass filters, to produce two coefficient subsets at each level (detailed and approximation coefficients). The frequency response of these filters is dependent on the type and the order of the mother wavelet $\Psi[n]$, chosen for the DWT analysis. Better decomposition is possible by increasing the order of the filter. The filtering operation usually continues until the desired level is reached. In this specific analysis, the Daubechies db3 mother wavelet is employed. As an illustrative example, when the decomposition level is set to 8, the DWT generates the coefficient subsets at this level details (cd1, cd2, cd3... and cd8) and approximation coefficient. The DWT output signals samples: cd1-cd3) waveform for channel number one is as shown in Fig. 6. The wavelet coefficient for each subset can be used as a feature for the corresponding muscle EMG signal. These individual wavelet components enable the straightforward extraction of the essential features that characterize the EMG signal.

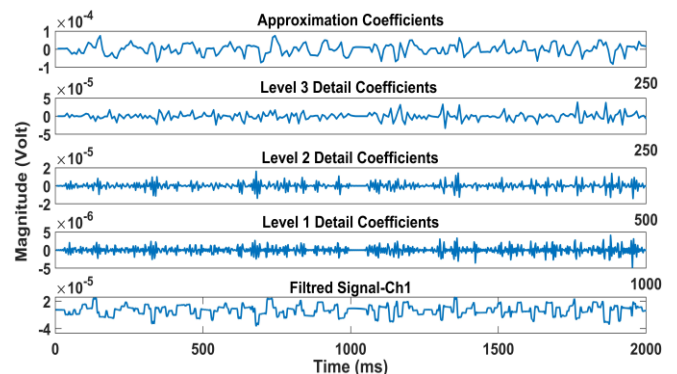


Fig. 6. DWT levels 1-3 for a single channel (channel1)

IV. CLASSIFICATION ALGORITHM

Regarding the architecture shown in Fig. 1, this section is dedicated to describing the main activities of the proposed algorithm which include three core steps; preprocessing, feature extraction, and post-processing (classification).

The algorithm steps: The algorithm comprises three essential processing phases: preprocessing, feature extraction, and post-processing. By preprocessing, the acquired EMG signal is reconditioned for processing in real-time application algorithms of prosthetic hand applications. Therefore, consecutive windowing of EMG signals in batches of data samples is adopted and a set of extracted features is evaluated. For each window, a set of features is computed to discern various movements. Subsequently, the classification stage takes charge of making decisions regarding movement predictions. This stage relies on the Feed Forward Back Propagation Neural Network (FFBPNN) classifier, specifically tailored for handling prediction tasks. The output of these stages is the predicted motion of the prosthetic hand as illustrated in Fig. 7.



Fig. 7. The proposed algorithm activity sequence

-Signal Preprocessing: The EMG signal exhibits an amplitude range of (0-10 mV peak-to-peak), with a (0-500 Hz) frequency, and a predominant power concentration within the 10 to 150 Hz frequency band. To enhance the signal's quality, the initial step involves subjecting the raw EMG signal to a band-pass filter ranging from 5 to 160 Hz. This filter effectively eliminates both unmarked signals and high-frequency noise, ensuring the purity of the data.

-Features Extraction: Time-domain (TD) features encompass energy-related attributes, demanding minimal computational resources. In contrast, frequency-domain (FD) features delve into the muscular activation power levels, necessitating a higher computational load. In real-time applications, computational load is a vital problem facing real-time activities. In order to overcome this problem, Xiao Feiyun [31] and Pengjie Qin [32] have used hardware circuits for real-time control of the upper-body exoskeleton. In this work, the DWT is adopted for feature extraction.

-Classification: The classifier performs an in-depth analysis of the features in the EMG signals (gestures). The input vector to the FFBPNN classifier is a set of FD features derived by the DWT to a certain level. The NN is structured by; an input layer that has a connection to the network's input vector, hidden layers that are fully connected with the adjacent layers, and the output layer that generates the classification scores for the seven motions (M1-M7) outlined in Table I. The misclassification problem may arise when two or more classes have very close values. It can be fixed, based on Linear Discriminant Analysis (LDA) method can be employed to refine the feature vector and improve classification accuracy [33, 34].

V. SYSTEM EXPERIMENTATION AND TESTING

This section dedicated to the testing, validation, and assessment of the algorithm. The primary parameters under evaluation are accuracy, response speed, and computational load, which are directly influenced by the degree of DWT, NN structure, and the number of hidden layers.

In order to assess the performance of the NN classifier the data set is partitioned into approximately 70% for training set and 30% for test set of the total observations. The performance of the NN classifier is evaluated by computing the test classification error. The classification accuracy of the FFNN is visualized in (n * n) confusion matrix (CM) for training, testing, and validation. The CM is presented in a tabular form, in which the rows correspond to the n actual classes, and the columns correspond to n predicted classes. Within this matrix, a comparison is made between the six actual target values and those predicted by the NN model. This is a powerful concept that offers a concise summary of the model's performance, highlighting instances of misclassification and offering guidance for improvement. As an example, the CM when cd=3 is shown in Fig.8.

		Training Confusion Matrix						
Output Class	1	700 15.0%	38 0.8%	155 3.3%	92 2.0%	1 0.0%	0 0.0%	71.0% 29.0%
	2	32 0.7%	532 11.4%	87 1.9%	19 0.4%	26 0.6%	15 0.3%	74.8% 25.2%
	3	13 0.3%	49 1.0%	412 8.8%	13 0.3%	28 0.6%	21 0.4%	76.9% 23.1%
	4	23 0.5%	35 0.7%	35 0.7%	556 11.9%	13 0.3%	10 0.2%	82.7% 17.3%
	5	16 0.3%	31 0.7%	34 0.7%	48 1.0%	708 15.2%	5 0.1%	84.1% 15.9%
	6	0 0.0%	60 0.3%	60 0.3%	36 0.8%	12 0.3%	754 16.3%	81.8% 18.2%
			89.3% 10.7%	71.4% 28.6%	52.6% 47.4%	72.8% 27.2%	89.8% 10.2%	93.7% 6.3%
		Target Class						
		Validation Confusion Matrix						
Output Class	1	162 16.2%	10 1.0%	34 3.4%	29 2.9%	0 0.0%	0 0.0%	68.9% 31.1%
	2	2 0.2%	103 10.3%	23 2.3%	2 0.2%	7 0.7%	2 0.2%	74% 25.9%
	3	4 0.4%	12 1.2%	76 7.6%	1 0.1%	3 0.3%	6 0.6%	74.5% 25.5%
	4	4 0.4%	16 1.6%	9 0.9%	110 11.0%	2 0.2%	2 0.2%	76.9% 23.1%
	5	6 0.6%	7 0.7%	8 0.8%	14 1.4%	146 14.6%	4 0.4%	78.9% 21.1%
	6	0 0.0%	16 1.6%	18 1.8%	6 0.6%	5 0.5%	152 15.2%	77.2% 22.8%
			91% 9.0%	62.8% 37.2%	45.2% 54.8%	67.9% 32.1%	89.6% 10.4%	91.6% 8.4%
		Target Class						
		Test Confusion Matrix						
Output Class	1	152 15.2%	10 1.0%	41 4.1%	19 1.9%	0 0.0%	0 0.0%	68.5% 31.5%
	2	8 0.8%	100 10.0%	16 1.6%	0 0.0%	11 1.1%	1 0.1%	71.5% 26.5%
	3	3 0.3%	12 1.2%	73 7.3%	2 0.2%	8 0.8%	3 0.3%	72.3% 27.7%
	4	2 0.2%	10 1.0%	6 0.6%	120 12.0%	2 0.2%	5 0.5%	82.8% 17.2%
	5	2 0.2%	10 1.0%	10 1.0%	14 1.4%	155 15.3%	0 0.0%	81.0% 19.0%
	6	0 0.0%	16 1.6%	14 1.4%	2 0.2%	4 0.4%	172 17.2%	82.7% 17.3%
			91.0% 9.0%	63.3% 36.7%	45.6% 54.4%	76.4% 23.6%	86.0% 14.0%	95.0% 5.0%
		Target Class						

All Confusion Matrix

		All Confusion Matrix							
		1	2	3	4	5	6	Accuracy	Loss
Output Class	1	1014 15.2%	58 0.9%	230 3.4%	140 2.1%	1 0.0%	0 0.0%	70.3%	29.7%
	2	42 0.6%	735 11.0%	126 1.9%	21 0.3%	44 0.7%	18 0.3%	74.5%	25.5%
	3	20 0.3%	73 1.1%	561 8.4%	16 0.2%	39 0.6%	30 0.4%	75.9%	24.1%
	4	29 0.4%	61 0.9%	50 0.7%	786 11.8%	17 0.3%	17 0.3%	81.9%	18.1%
	5	24 0.4%	48 0.7%	52 0.8%	76 1.1%	1007 15.1%	9 0.1%	82.8%	17.2%
	6	0 0.0%	92 1.4%	92 1.4%	44 0.7%	21 0.3%	1078 16.2%	81.2%	18.8%
		89.8% 10.2%	68.9% 31.1%	50.5% 49.5%	72.6% 27.4%	89.2% 0.8%	93.6% 6.4%	77.7% 22.3%	
		1	2	3	4	5	6		
		Target Class							

Fig. 8. Confusion matrices for classification (cd=3)

While the CM enables predictions for specific classes, it does not address the practical challenge of ranking different classes based on their performance to identify the best one. The CM can facilitate the calculation of various performance metrics, including the misclassification error, which quantifies the ratio of incorrectly classified instances to the total instances, and accuracy, determined by the ratio of correctly classified instances to the total measured instances [35, 36].

$$accuracy = \frac{TP+TN}{FP+FN+TP+TN} \tag{5}$$

Where the terminology:

- TP (True Positive): Instances that are correctly classified as positive.
- TN (True Negative): Instances that are correctly classified as negative.
- FP (False Positive): Instances that are incorrectly classified as positive.
- FN (False Negative): Instances that are incorrectly classified as negative.

Additionally, there are other important metrics to consider, such as precision, recall, and specificity. Precision measures the ratio of correctly classified instances against the total predicted instances for a specific class. These metrics are expressed in formulas (6) and (7) respectively.

$$precision (positive) = \frac{TP}{FP+TP} \tag{6}$$

$$precision (negative) = \frac{TN}{FN+TN} \tag{7}$$

The recall, in classification measures the ratio of correctly classified instances to the total number of instances. False positive rate (specificity) is denoted as the ratio of instances incorrectly classified as positive to all negative instances. Similarly, positive recall and sensitivity refer to the same concept, which is the ability to correctly identify positive cases. The positive and negative recall is stated in formulas (8) and (9) respectively:

$$Sensitivity = Recall (positive) = \frac{TP}{FN+TP} \tag{8}$$

$$Specificity = Recall (negative) = \frac{TN}{FP+TN} \tag{9}$$

The three metrics (accuracy, specificity, and precision) are reasonable measures for the performance of the classifier. For evaluation, comprehensive measures employed, some of which trying to combine two complementary indicators into single metric, such as the F-measure, defined as the harmonic mean of the precision and recall indicators [37, 38]. Both misclassification error and accuracy serve as class-insensitive performance measures, basically presenting the same information. These performance metrics directly reflect how well the classifier identifies the true class correctly. Therefore, there is no need to use them simultaneously, as doing so would result in informational redundancy.

Table II, illustrates the accuracy for different NNs, namely (PatternNet, FitNet, FFNet, and CascadeForwardNet) corresponding to the number of DWT levels: 3, 4, 5, 6, 7, and 8 as well as the average of all 6 levels when implemented in parallel for each type of NN. The input dataset is randomly divided into 70% for training (Tr), 30% for testing (Te), and validation (Va). The training process is limited to a maximum of 1000 epochs, employing the "Tansigmoid" training function and assessing performance using the "MSE" (Mean Squared Error) performance function to control the networks.

TABLE II
THE MEAN RECOGNITION ACCURACY (Ac) VALUE OF NNS
CORRESPONDING TO DWT LEVELS (cd3- cd8).
TrAc-training accuracy, VaAc-validation accuracy, TeAc-testing accuracy

NN		cd3	cd4	cd5	cd6	cd7	cd8
Pattern NN	TrAc	78.4	64.8	78.2	88.4	88.9	90.3
	VaAc	74.8	63.6	73.9	85.9	75.3	78.6
	TeAc	76.9	61.1	77.0	80.0	86.3	88.1
Fit NN	TrAc	87.9	81.5	78.3	68.8	83.3	87.5
	VaAc	82.7	73.5	75.5	70.4	79.7	84.8
	TeAc	80.4	76.7	77.0	74.1	87.7	80.0
FFNN	TrAc	86.9	91.7	88.0	90.8	91.2	90.8
	VaAc	83.1	84.4	83.1	83.0	86.3	76.2
	TeAc	81.9	84.4	82.4	82.2	84.9	90.5
cascade FNN	TrAc	68.2	60.9	64.3	70.4	91.8	90.3
	VaAc	64.4	60.1	68.2	64.4	93.7	78.6
	TeAc	60.8	62.3	60.5	70.4	82.6	81.0

The DWT decomposition is evaluated with the maximum depth limited to 8 levels. To examine the significance of each level, we conducted many experiments by varying the number of levels and testing the resulting confusion matrices.

The NN model we have adopted constructed of five hidden layers, and the number of neurons in each layer is fixed empirically by varying and tuning them. For L-level wavelet decomposition, the extracted features are obtained from F feature extraction functions and result in (L+1)×F features. The output layer of the network consists of 6 neurons, each one assigned to a unique class. In each layer of the NN, the activation function used is Tangent Sigmoid, with the exception of the final layer, which utilizes the Softmax function. A sample for the FFNN data classification performance is shown in Fig. 9.

The assessment of (PatternNet, FitNet, FFNet, and CascadeForwardNet) performance is conducted by varying

the levels of DWT (3, 4, 5, 6, 7, and 8) and evaluating the mean squared error stopping criteria, which is a reliable metric of the accuracy, as demonstrated in Table III.

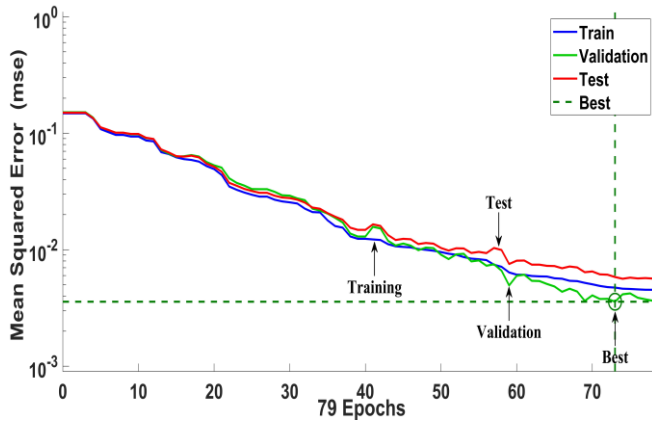


Fig. 9. The FFNN (8-28-64-32-16-8-6) performance in data classification.

TABLE III

THE NNS PERFORMANCE CORRESPONDINGS TO DWT (cd3- cd8)
TrP-training performance, VaP-validation performance,
TeP-testing performance.

NN	DWT levels	cd3	cd4	cd5	cd6	cd7	cd8
		Pattern NN	TrP	0.0554	0.0823	0.0563	0.0483
	VaP	0.0601	0.0835	0.0616	0.0571	0.0503	0.0252
	TeP	0.0582	0.0887	0.0565	0.0579	0.0347	0.0335
	Grad.	0.0525	0.0645	0.0553	0.127	0.0468	0.0484
Fit NN	TrP	0.038	0.0521	0.0618	0.0767	0.039	0.0123
	VaP	0.0507	0.0649	0.0659	0.0725	0.0514	0.0221
	TeP	0.0531	0.0645	0.0591	0.0743	0.0415	0.0406
	Grad.	0.0452	0.1210	0.1140	0.0600	0.0462	0.0146
FFNN	TrP	0.0411	0.0306	0.0393	0.0156	0.0332	0.0511
	VaP	0.0496	0.0491	0.053	0.0767	0.0364	0.0584
	TeP	0.0525	0.0456	0.0513	0.0687	0.0476	0.0497
	Grad.	0.0919	0.0593	0.0845	0.0465	0.1501	0.0062
Cascade FNN	TrP	0.1093	0.1021	0.0976	0.0821	0.0339	0.0528
	VaP	0.0977	0.1032	0.1077	0.0973	0.0488	0.2145
	TeP	0.1093	0.1038	0.1091	0.0981	0.0787	0.1660
	Grad.	0.3400	0.2760	0.3390	0.7210	0.2840	0.0470

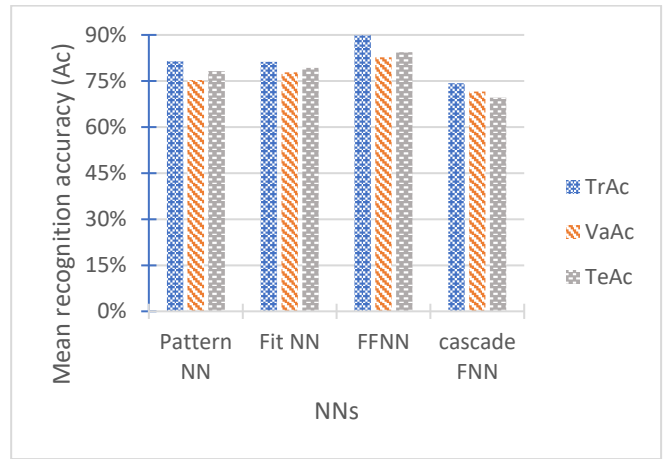
Table IV contains the accuracy values obtained through testing EMG signals under specific conditions. In this test, the input data is distorted by a random noise on selected channel signals to simulate hardware errors and muscle dysfunction. The signals are deliberately contaminated using a random noise model that is adjusted to closely mimic real-world noise parameters, that characterized by the parameters; SNR (Signal-to-Noise Ratio) set at 45 dB, standard deviation (SD) equal to 5, and mean (μ) at 0.0.

TABLE IV

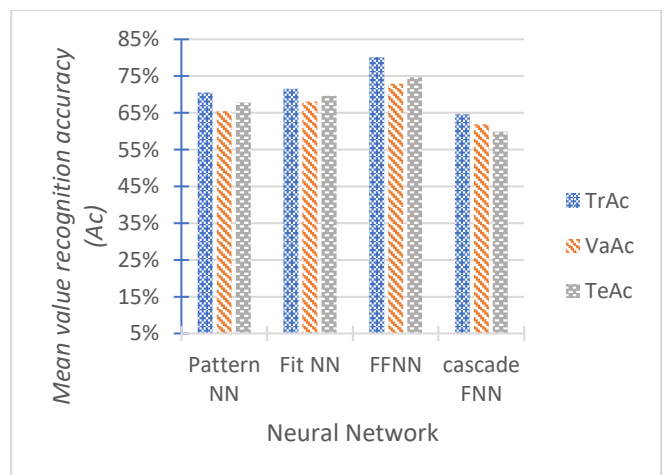
THE MEAN VALUE RECOGNITION ACCURACY (AC) FOR EMG SIGNALS CORRUPTED BY NOISE (SNR=45dB, $\sigma =5$, $\mu=0.0$).
TrAc-training accuracy, VaAc-validation accuracy, TeAc-testing accuracy

		DWT Levels					
NN		cd3	cd4	cd5	cd6	cd7	cd8
Pattern NN	TrAc	66.9	55.1	68.5	78.7	79.2	80.6
	VaAc	64.2	53.9	64.2	76.2	65.6	68.9
	TeAc	62.7	51.4	67.3	70.3	76.6	78.4
Fit NN	TrAc	78.2	71.8	68.6	59.1	73.6	77.8
	VaAc	73.0	63.8	65.8	60.7	70.0	75.1
	TeAc	70.7	67.0	67.3	64.4	78.0	70.3
FFNN	TrAc	77.2	82.0	78.3	81.1	81.5	81.1
	VaAc	73.4	74.7	73.4	73.3	76.6	66.5
	TeAc	72.2	74.7	72.7	72.5	75.2	80.8
Cascade FNN	TrAc	58.5	51.2	54.6	60.7	82.1	80.6
	VaAc	54.7	50.4	58.5	54.7	84.0	68.9
	TeAc	51.1	52.6	50.8	60.7	72.9	71.3

The mean performance accuracy for each type of neural network, with the highest values in terms of (Training Accuracy, Validation Accuracy, and Testing Accuracy) achieved by the FFNN is as illustrated in Fig.10-a.



(10-a)



(10-b)

Fig. 10. The mean accuracy of (TrAc, VaAc, TeAc) for different NNs. (a) without noise, (b) when the EMG signal has additive noise; SNR=45 dB, SD =5, and $\mu=0.0$.

By analyzing the results, it becomes evident that the neural network's performance has a direct impact on the overall performance of the recognition system. Even in the presence of noise in the EMG signal, the system still maintains a relatively high level of performance. Moreover, the FFNN consistently outperforms other neural networks, displaying superior mean accuracy values of (Training Accuracy = 8.7%, Validation Accuracy = 4.17%, and Testing Accuracy = 5.06%) compared to the nearest competitor in mean accuracy performance. This performance difference is clearly demonstrated in Fig. 10-b, which shows the accuracy using different NNs when the EMG signal is corrupted by additive noise characterized by; SNR = 45 dB, SD = 5, and $\mu = 0.0$.

VI. DISCUSSION AND FUTURE WORK

Based on the analysis of the results, it becomes evident that the filtering process plays a crucial role in noise reduction and eliminating redundant data. Figures 3 and 4 underscore the significance of low-frequency components in EMG signal information, while also indicating that higher-frequency components carry minimal relevant information that may be safely disregarded. Consequently, a low-frequency bandpass filter was employed to select the informative signals.

The utilization Confusion Matrix (CM) is an effective concept for assessing performance, as it involves comparing actual target value with predictions made by the machine learning model. Tables II and III demonstrate a direct correlation between classification accuracy and the number of DWT levels, showing a sensible improvement as the number of levels increases. The highest average accuracy of 89.9% is achieved by training the FFNN. The performance of other neural networks is also presented in the aforementioned tables, where structural adjustments are explored and practically tested to enhance performance.

In conclusion, it is imperative to make some notes about the limitations facing this work, and the proposed solutions for development. The first point is that the pattern recognition of the EMG data is adopted only in offline applications, thus the participants (both healthy and amputee subjects) are neither tested in real-time nor in a simulated environment. Functional testing is performed to check the usability, validity, and classification accuracy of a given hand movement or gesture. However, more extensive research on larger and more diverse datasets may yield even better performance results. A second point is, the algorithm primarily focused on single-hand movements, excluding wrist, arm, or finger movements (compound movements). This limitation could introduce confusion and interference between various movements, as well as considerations for limb position and forearm orientation. One more point that may be an added value to the research, is expanding the number of cases (especially amputee persons) demonstrating the same functions. The results show that algorithm performance improves with a smaller set of movements and a larger pool of subjects.

VII. CONCLUSIONS

This paper presents a comprehensive investigation into the utilization of surface electromyography (sEMG) signals for

the precise identification of individual hand movements and dexterous prosthetic control. This research also contributes to the development of real-time control mechanisms for prosthetic hands and electric-powered wheelchairs. Experimental results reported the crucial role of the discrete wavelet transform (DWT) in extracting features from EMG signals and subsequent motion recognition using neural networks (NNs). Specifically, the results underscore the efficacy of the system in accurately identifying various hand movements, with a remarkable maximum average accuracy of 89.9%.

Practical analysis reveals that augmenting the components within low-frequency and high-frequency EMG signals does not yield a significant improve in the accuracy of identifying multiple classes. Instead, it emphasizes the importance of carefully selecting the cut-off frequency and sampling rate to ensure high classification accuracy, which directly impacting the performance of myoelectric prosthesis control. A filter range of 5-160Hz looks to be an appropriate choice for EMG signals filtering in hand movement classification. The average classification performance depends on the number of DWT features incorporated. Augmenting additional number of DWT features generally enhances the classification rate, although there is a limited statistical change in accuracy when including features in higher DWT levels.

The confusion matrix (CM) provides a direct measure of classification error, identifying instances where one type of gesture is confused with another gesture. Four different types of neural networks were employed and evaluated using the same datasets, exhibiting that the feedforward neural network (FFNN) has a superior performance in terms of accurate classification compared to other NNs.

From a practical engineering standpoint, the design of prosthetic control architecture should prioritize simplicity to facilitate implementation. Therefore, the development of an efficient, low-encumbrance, gesture-based control system is imperative for optimizing the functionality of prosthetic devices.

REFERENCES

- [1] O. Fukuda, T. Tsuji, M. Kaneko, and A. Otsuka, "A human-assisting manipulator teleoperated by EMG signals and arm motions.," *IEEE Transactions on Robotics and Automation*, vol. 19, no. 2, pp. 210-222, 2003.
- [2] T. Luhandjula, K. Djouani, Y. Hamam, B. van Wyk, and Q. Williams, "A hand-based visual intent recognition algorithm for wheelchair motion.," In: *3rd International Conference on Human System Interaction, HSI'2010 - Conference Proceedings*, pp. 749-756, 2010.
- [3] R.Z. Khan and N.A. Ibraheem, "Survey on Gesture Recognition for Hand Image Postures.," *Computer and Information Science*, vol. 5, no. 3, pp. 110-121, 2012.
- [4] J.J.V. Mayor, R.M. Costa, A. Frizzera Neto, and T.F. Bastos, "Dexterous hand gestures recognition based on low-density sEMG signals for upper-limb forearm amputees.," *Research on Biomedical Engineering*, vol. 33, no. 3, pp. 202-217, 2017.
- [5] G. Li, Y. Li, L. Yu, and Y. Geng, "Conditioning and sampling issues of EMG signals in motion recognition of multifunctional myoelectric prostheses.," *Annals of Biomedical Engineering*, vol. 39, no. 6, pp.1779-1787, 2011.
- [6] K.L. Lew, K.S. Sim, S.C. Tan, and F.S. Abas, "Biofeedback Upper Limb Assessment Using Electroencephalogram, Electromyographic and Electrocardiographic with Machine Learning in Signal Classification.," *Engineering Letters*, vol. 30, no. 3, pp. 935-947, 2022.
- [7] R. Boostani and M.H. Moradi, "Evaluation of the forearm EMG signal features for the control of a prosthetic hand.," In: *Physiological Measurement*, Vol.24, no. 2, pp.309-319, 2003.

- [8] B. Karlik, "Machine Learning Algorithms for Characterization of EMG Signals," *International Journal of Information and Electronics Engineering*, vol. 4, no. 3, pp. 189-194, 2014.
- [9] A. Phinyomark, R.N. Khushaba, and E. Scheme, "Feature extraction and selection for myoelectric control based on wearable EMG sensors.," *Sensors*, vol. 18, no. 5, pp. 1615-1631, 2018.
- [10] P. Visconti, F. Gaetani, G.A. Zappatore, and P. Primiceri, "Technical features and functionalities of Myo Armband: An overview on related literature and advanced applications of myoelectric armbands mainly focused on arm prostheses.," *International Journal on Smart Sensing and Intelligent Systems*, vol. 11, no. 1, pp. 1-25, 2018.
- [11] U. Côté-Allard, G. Gagnon-Turcotte, F. Laviolette, and B. Gosselin, "A low-cost, wireless, 3-D-printed custom armband for sEMG hand gesture recognition.," *Sensors*, vol. 19, no. 12, pp. 2811-2834, 2019.
- [12] M.W. Jiang, R.C. Wang, J.Z. Wang, and D.W. Jin, "A method of recognizing finger motion using wavelet transform of surface EMG signal.," In: *Annual International Conference of the IEEE Engineering in Medicine and Biology – Proceedings*, pp. 2672-2674, 2005.
- [13] G.R. Naik, S. Arjunan, and D. Kumar, "Applications of ICA and fractal dimension in sEMG signal processing for subtle movement analysis: A review.," *Australasian physical & engineering sciences in medicine*, vol. 34, no. 2, pp. 179-193, 2011.
- [14] A.H. Al-Timemy, G. Bugmann, J. Escudero, and N. Outram, "Classification of finger movements for the dexterous hand prosthesis control with surface electromyography.," *IEEE Journal of Biomedical and Health Informatics*, vol. 17, no. 3, pp. 608-618, 2013.
- [15] F. Sebelius, L. Eriksson, C. Balkenius, and T. Laurell, "Myoelectric control of a computer animated hand: A new concept based on the combined use of a tree-structured artificial neural network and a data glove.," *Journal of Medical Engineering and Technology*, vol. 30, no. 1, pp. 2-10, 2006.
- [16] J.L. Pons, R. Ceres, E. Rocon, et al., "Virtual reality training and EMG control of the MANUS hand prosthesis.," *Robotica*, vol. 23, no. 3, pp. 311-317, 2005.
- [17] S. Herle, P. Raica, G. Lazea, R. Robotin, C. Marcu, and L. Tamas, "Classification of surface electromyographic signals for control of upper limb virtual prosthesis using time-domain features.," In: *2008 IEEE International Conference on Automation, Quality and Testing, Robotics*, vol. 3, pp. 160-165, 2008.
- [18] A.D. Keleş and C.A. Yucesoy, "Development of a neural network-based control algorithm for powered ankle prosthesis.," *Journal of Biomechanics*, vol. 113, p. 110087, 2020.
- [19] E. Lamounier, K. Lopes, A. Cardoso, A. Andrade, and A. Soares, "On the use of Virtual and Augmented Reality for upper limb prostheses training and simulation.," *Annual International Conference of the IEEE Engineering in Medicine and Biology Society, EMBC'10*, pp.2451-2454, 2010.
- [20] F.E.R. Mattioli, E.A. Lamounier, A. Cardoso, A.B. Soares, and A.O. Andrade, "Classification of EMG signals using artificial neural networks for virtual hand prosthesis control.," *Proceedings of the Annual International Conference of the IEEE Engineering in Medicine and Biology Society, EMBS*, pp. 7254-7257, 2011.
- [21] R.B. Azhiri, M. Esmaili, and M. Nourani, "EMG-Based Feature Extraction and Classification foProsthetic Hand Control.," *EPiC Series in Computing*, vol. 83, pp. 136-145, 2022.
- [22] S. Lobov, N. Krilova, I. Kastalskiy, V. Kazantsev, and V.A. Makarov, "Latent factors limiting the performance of sEMG-interfaces.," *Sensors*, vol. 18, no. 4, pp. 1-19, 2018.
- [23] U. Ozkaya, O. Coskun, and S. Comlekci, "Frequency analysis of EMG signals with Matlab spool.," *WSEAS International Conference on Signal Processing, SIP '10*, pp. 83-88, 2010.
- [24] C.J. de Luca, L. Donald Gilmore, M. Kuznetsov, and S.H. Roy, "Filtering the surface EMG signal: Movement artifact and baseline noise contamination.," *Journal of Biomechanics*, vol. 43, no. 8, pp.1573-1579, 2010.
- [25] L. St. George, S.H. Roy, J. Richards, J. Sinclair, and S.J. Hobbs, "Surface EMG signal normalisation and filtering improves sensitivity of equine gait analysis.," *Comparative Exercise Physiology*, vol. 15, no. 3, pp. 173-185, 2019.
- [26] P.C. Bhaskar and M.D. Uplane, "High Frequency Electromyogram Noise Removal from Electrocardiogram Using FIR Low Pass Filter Based on FPGA.," *Procedia Technology*, vol. 25, pp. 497-504, 2016.
- [27] D. Nieto, J.D. Martinez-Vargas, and E. Giraldo, "Multirate Adaptive Filter Banks based on Automatic Bands Selection for Epilepsy Detection.," *Engineering Letters*, vol. 29, no. 1, pp. 43-48, 2021.
- [28] D. M. Ballestros, A. E. Gaona, and L. F. pedraza, "Discrete Wavelet Transform in Compression and Filtering of Biomedical Signals.," *Discrete Wavelet Transforms - Biomedical Applications*, 2011.
- [29] E.L. Lema-Condo, F.L. Bueno-Palomeque, S.E. Castro-Villalobos, E.F. Ordonez-Morales, and L.J. Serpa-Andrade, "Comparison of wavelet transform symlets (2-10) and daubechies (2-10) for an electroencephalographic signal analysis.," In: *Proceedings of the 2017 IEEE 24th International Congress on Electronics, Electrical Engineering and Computing, INTERCON*, pp. 1-4, 2017.
- [30] R. Madan, P. Sunil, K. Singh, and N. Jain, "Signal Filtering Using Discrete Wavelet Transform.," *International Journal of Recent Trends in Engineering*, vol. 2, no. 3, pp. 96-98, 2009.
- [31] F. Xiao, J. Mu, J. Lu, G. Dong, and Y. Wang, "Real-time modeling and feature extraction method of surface electromyography signal for hand movement classification based on oscillatory theory.," *Journal of Neural Engineering*, vol. 19, no. 2, p. 026011, 2022.
- [32] P. Qin and X. Shi, "Evaluation of feature extraction and classification for lower limb motion based on sEMG signal.," *Entropy*, vol. 22, no. 8, p. 852-863, 2020.
- [33] A.J. Izenman, "Linear discriminant analysis.," In *Modern multivariate statistical techniques*, Springer, pp. 237-280, 2013.
- [34] X.-J. Zhang, X.-C. Zhu, D. Wu, Z.-Z. Xiao, Z. Tao, and H.-M. Zhao, "Nonlinear Features of Bark Wavelet Sub-band Filtering for Pathological Voice Recognition.," *Engineering Letters*, vol. 29, no. 1, pp. 49-60, 2021.
- [35] S.E. Buttrey, "Data Mining Algorithms Explained Using R.," *Journal of Statistical Software*, vol. 66, no. Book Review 2, pp. 683-686, 2015.
- [36] A.M. Ceballos-Arroyo, S. Robles-Serrano, and G. Sanchez-Torres, "A morphological convolutional autoencoder for segmenting pigmented skin lesions.," *Engineering Letters*, vol. 28, no. 3, pp. 855-866, 2020.
- [37] N.F. Shamsudin, H. Basiron, Z. Saaya, A.F.N. Abdul Rahman, M.H. Zakaria, and N. Hassim, "Sentiment classification of unstructured data using lexical based techniques.," *Jurnal Teknologi*, vol. 77, no. 18, pp.113-120, 2015.
- [38] A. Subasi, "Biomedical Signal Processing Techniques.," In: *Practical Guide for Biomedical Signals Analysis Using Machine Learning Techniques*, Academic press, pp. 89-190, 2019.